

This is the **accepted version** of the journal article:

Okada, M.; Yang, Z.; Mas, P. «Circadian autonomy and rhythmic precision of the Arabidopsis female reproductive organ». *Developmental Cell*, Vol. 57 Núm. 18 (26 2022), p. 2168-2180.e4. DOI 10.1016/j.devcel.2022.08.013

This version is available at <https://ddd.uab.cat/record/273537>

under the terms of the  ^{IN}
COPYRIGHT license

Circadian autonomy and rhythmic precision of the Arabidopsis female reproductive organ

Masaaki Okada^{1,3}, Zhiyuan Yang^{1,3}, Paloma Mas^{1, 2, 4*}

¹Centre for Research in Agricultural Genomics (CRAG), CSIC-IRTA-UAB-UB, Campus UAB, Bellaterra, 08193 Barcelona, Spain.

²Consejo Superior de Investigaciones Científicas (CSIC), 08028 Barcelona, Spain.

³These authors contributed equally to the manuscript

⁴Lead contact

*Correspondence to: paloma.mas@cragenomica.es

Further information and requests for resources and reagents should be directed to and will be fulfilled by the lead contact, Paloma Mas (paloma.mas@cragenomica.es).

SUMMARY

The plant circadian clock regulates essential biological processes including flowering time or petal movement. However, little is known about how the clock functions in flowers. Here we identified the circadian components and transcriptional networks contributing to the generation of rhythms in pistils, the female reproductive organ. When detached from the rest of the flower, pistils sustain highly precise rhythms, indicating organ-specific circadian autonomy. Analyses of clock mutants and chromatin immunoprecipitation assays showed distinct expression patterns and specific regulatory functions for clock activators and repressors in pistils. Genetic interaction studies also suggested a hierarchy of the repressing activities that provide robustness and precision to the pistil clock. Globally, the circadian function in pistils primarily governs responses to environmental stimuli and photosynthesis, and controls pistil growth and seed weight and production. Understanding the circadian intricacies in reproductive organs may prove useful for optimizing plant reproduction and productivity.

INTRODUCTION

The circadian clock generates 24-h biological rhythms in synchrony with external and internal cues (Young and Kay, 2001). At its basis, generation of the rhythms relies on a precise rhythmic regulation of clock gene expression and protein function (Chen and Mas, 2019; Crosby and Partch, 2020; Seo and Mas, 2014; Takahashi, 2017). The circadian molecular network has been extensively investigated

in the model plant *Arabidopsis thaliana*, most notably using whole seedlings (Nakamichi, 2020). Recent studies on specific organs and tissues are uncovering both the circadian autonomy of some organs (e.g. Thain et al., 2000, 2002; James et al., 2008; Yakir et al., 2011; Fukuda et al., 2012; Wenden et al., 2012; Endo et al., 2014; Bordage et al., 2016) as well as the coupling and coordination of rhythms within the plant (Chen et al., 2020; Endo et al., 2014; Fukuda et al., 2007; Gould et al., 2018; Greenwood et al., 2019; Takahashi et al., 2015). Therefore, the plant circadian system comprises autonomous tissue-specific rhythms complemented with cell-to-cell coupling and long distance coordination (Nakamichi, 2020; Sorkin and Nusinow, 2021).

Transcriptional feedback loops at the core of the *Arabidopsis* oscillator delineate a time-of-day specific expression of the main oscillator genes (McClung, 2019; Nakamichi, 2020; Sanchez and Kay, 2016). The morning-expressed core clock components include the single-MYB transcription factors CCA1 (CIRCADIAN CLOCK ASSOCIATED1), LHY (LATE ELONGATED HYPOCOTYL) and the members of the PRR (PSEUDO-RESPONSE REGULATOR) family, PRR9 and PRR7, which act during the day primarily to repress clock gene expression (McClung, 2019; Nakamichi, 2020; Sanchez and Kay, 2016). Core clock components expressed close to dusk or at night include additional members of the PRR family, such as PRR5 and TOC1/PRR1 (TIMING OF CAB EXPRESSION1/PSEUDO RESPONSE REGULATOR1) as well as the components of the Evening Complex (EC), comprising ELF3 (EARLY FLOWERING 3), ELF4 and LUX/PCL1 (LUX ARRHYTHMO/ PHYTOCLOCK1) (McClung, 2019; Nagel and Kay, 2012; Nakamichi, 2020). The evening-expressed components function as repressors of morning genes to ensure that they are repressed during the night.

In addition to the clock repressors, several activators shape the rhythmic oscillations. Some of the activators include chromatin marks contributing to an open chromatin conformation (Chen and Mas, 2019) and additional clock components such as LWD1 and 2 (LIGHT-REGULATED WD1 and 2) (Wang et al., 2011; Wu et al., 2008, 2016), or members of the RVE (REVEILLE) protein family (Farinas and Mas, 2011; Hsu et al., 2013; Rawat et al., 2011; Shalit-Kaneh et al., 2018). The RVE proteins form a co-activating protein complex with the LNK (NIGHT LIGHT-INDUCIBLE AND CLOCK-REGULATED GENE) proteins (Ma et al., 2018; Rugnone et al., 2013; Xie et al., 2014) and activate clock gene expression by timely recruiting the transcriptional machinery to control the rhythms of nascent RNAs (Ma et al., 2018). Altogether, current models of the *Arabidopsis* oscillator depict the transcriptional regulation of morning-expressed clock components that specifically regulate evening clock genes and vice versa (Avello et al., 2021; Caluwé et al., 2016).

The time-of-day specific expression of oscillator genes and proteins defines the timing of biological processes or outputs controlled by the clock. The circadian clock intersects with the function of major organelles and cellular pathways including among many others, hormonal pathways (Sanchez and Kay, 2016), the cell cycle (Fung-Uceda et al., 2018), chloroplasts (Atkins and Dodd, 2014; Flis et al., 2019; Fukushima et al., 2009) or mitochondria (Cervela-Cardona et al., 2021; Fukushima et al., 2009; Sanchez-Villarreal et al., 2013). Consequently, the circadian system regulates nearly every aspect of development, growth, metabolism and responses to biotic and abiotic stresses (Adams and Carré, 2011; Kinmonth-Schultz et al., 2013; Sanchez and Kay, 2016). The photoperiodic regulation of flowering time has been firmly established as an important clock output (Shim et al., 2017). Daily rhythms of scent emission, pollinator attraction, flower closing and orientation have been also documented (Atamian et al., 2016; Creux et al., 2021; Fenske and Imaizumi, 2016; Fenske et al., 2018; Muroya et al., 2021). However, there is limited information about how the clock actually works in flowers and what specific molecular and cellular pathways regulates within the flower.

Arabidopsis flowers show the typical structure of the *Brassicaceae*, which consist of concentric whorls, including four sepals, a corolla of four petals, the androecium with six stamens, and the gynoecium at the center (Drews et al., 1991; Sablowski, 2015; Weigel, 1995; Wellmer et al., 2014). The gynoecium contains two fused carpels separated by a false septum that divide the ovary into two compartments (Ferrándiz et al., 1999; Zúñiga-Mayo et al., 2019). The gynoecium allows pollen fertilization of the ovules, which eventually will develop into seeds. Here we have studied the circadian function in flowers and reproductive organs and identified the specific regulatory network at the core of the clock in pistils, arguably one of the more complex and evolutionary innovative organs of flowering plants (Simonini and Østergaard, 2019). We found a distinct functional network that confers precision and robustness to the pistil clock.

RESULTS

Self-sustained circadian rhythms in detached buds and flowers

To understand the circadian clock function in floral organs, we examined rhythms in buds and flowers at different developmental stages (Figure 1A). Young and mature buds (stages 6-12) (Müller, 1961; Smyth et al., 1990) sustained high-amplitude and robust circadian rhythms of *CCA1:LUC* activity (*CCA1* promoter fused to the LUCIFERASE) with circadian periods close to 24 h under constant light (LL) conditions (Figure 1B-C). Mature and fully open flowers (stages 13-15) (Müller, 1961;

Smyth et al., 1990) also sustained rhythms under both LL (Figure 1D-E) and entraining conditions (Figure S1A). Evening-phased circadian reporters such as *TOC1::LUC* and *GIGANTEA::LUC* (*GI::LUC*) also showed high-amplitude rhythms in flowers (Figure S1B-F). Consistent with the bioluminescence results, RT-QPCR (Reverse Transcription-Quantitative Polymerase Chain Reaction) analyses confirmed the rhythmic circadian expression of oscillator genes in flowers (Figure 1F-G). Thus, a functional circadian clock sustains rhythms in buds and flowers detached from the rest of the plant, although the rhythmic oscillations appeared more robust in buds than in flowers.

Analyses of circadian rhythms in *toc1-2* mutant showed that *toc1-2* buds sustained the rhythmic oscillations, albeit with a short period (~ 20 h) (Figure 2A-C), and thus, displaying a phenotype similar to that previously reported in seedlings (Millar et al., 1995). In flowers, *toc1-2* showed short-period oscillations only the first two or three days, dampening low afterwards (Figure 2D-F) (higher Relative Amplitude Error values indicate weaker rhythms). Comparative analyses confirmed the altered *toc1-2* rhythms in flowers compared to buds (Figure 2G-H). Altogether, the circadian phenotype of *toc1-2* buds resembles that previously reported in seedlings, but rhythms dampen low after few days in *toc1-2* flowers.

Detached female reproductive organs show precise and robust rhythms

Variations of rhythms in the different floral organs can contribute to the rhythmic dampening in *toc1-2* flowers. Thus, we examined the circadian oscillation in sepals, petals, stamens and pistils (Figure 3A). In WT sepals, bioluminescence rhythms were robustly sustained, albeit with a shorter period than 24 h (Figure 3B, H). Rhythms in WT petals and stamens showed short circadian periods for three or four days, dampening low afterward (Figure 3C, D, I, and Figure S2A-B). In contrast, the circadian waveforms in pistils robustly oscillated for more than five days, with a circadian period close to 24 h (Figure 3E-H, J). We observed similar results with different clock reporters (Figure S2C-F). Time course analyses by RT-QPCR also confirmed the differences observed between stamens and pistils (Figure S2G-H). When we followed individual open flowers in intact plants that were maintained for several days under LL, we found that apart from pistils, the other floral organs disappeared very rapidly, indicating that floral organs other than pistils are short-lived in planta (Figure S2I). Therefore, reduced viability and/or the lack of energy after excision might contribute to the dampening of the rhythms that we observed in the bioluminescence assays. In any case, our results showed that pistils can survive for several days after excision from the rest of the flower and that the circadian rhythms in pistils robustly oscillate. Fertilization appears not to be a major factor contributing to the robustness

of the pistil clock as similar patterns of gene expression were observed in pistils from flowers before and after fertilization (Figure S2J-M).

In *toc1-2* sepals, rhythms were similar to WT for the first three days, albeit with slightly reduced amplitude. Thus, the characteristic short-period phenotype of *toc1-2* observed in seedlings and buds was only evident in sepals after several days under LL (Figure 3B, and Figure S3A). We observed a similar trend in *toc1-2* petals and stamens although the dampened rhythms precluded a clear view of the possible period shortening over time (Figure 3C, D, and Figure S3B, C). As mentioned above, the reduced viability or the lack of energy might contribute to the dampening of the rhythms. In any case, analyses of rhythms at early time points before dampening showed that the circadian period of *toc1-2* sepals and petals was not significantly different from WT, whereas the circadian period of *toc1-2* stamens was significantly longer than WT (p-value 0.0003 in samples with RAE<0.4). In pistils, the short-period oscillation observed during the first day rapidly transitioned to very-low amplitude rhythms (Figure 3E and Figure S3D), following a similar trend to that observed in whole flowers. Comparison of the different floral organs revealed the organ-specific behavior of *toc1-2* mutant (Figure S3E, F).

The pistil clock regulates the circadian expression of genes involved in photosynthesis and responses to stimuli, and controls pistil growth and seed production

We next performed time course analyses by RNA sequencing (RNA-seq) to obtain a genome-wide view of the circadian transcriptional landscape in pistils. We first verified the reliability of the RNA-seq data by comparing our dataset with a previously published analysis of pistil-enriched genes (Klepikova et al., 2016; Martínez-Fernández et al., 2014). Initial comparisons revealed that the similarities were high despite the different sampling, growing conditions, and mode of analyses (Figure S4A). For example, the highest and lowest expressed genes were highly conserved in both datasets (examples in Figure S4B). The trends of expression for many of the genes was also quite similar (Figure S4C-D and E-F). We also found that the expression of genes characteristic of other floral organs was absent or much reduced compared to canonical pistil genes (Figure S4G) suggesting that our dataset was specific and reliably reflected the transcriptional landscape in pistils.

Analyses of the rhythmic genes in pistils using the JTK_CYCLE algorithm (Hughes et al., 2010) (adjusted p-value <0.05) uncovered around 1000 circadian genes (Table S1) with a range of amplitudes that were similar or slightly lower than the ones previously described at the shoot apex (Takahashi et al., 2015) (Figure 4A-B). Overall, low-amplitude rhythmic genes showed lower

expression than high-amplitude genes (Figure S4H). The circadian phases of rhythmic genes in pistils expanded across the whole circadian cycle but were slightly enriched during the day, particularly at Circadian Time 4 (CT4) (Figure 4C) as opposed to the enrichment after subjective dusk observed at the shoot apex (Takahashi et al., 2015) (Figure S4I). In addition to the organ-specificities, different entrainment regimes (pistils: 16h light: 8h dark versus shoot apices: 12h light: 12h dark) can contribute to peak-phase differences.

Functional categorization of the rhythmic genes showed significant enrichment in photosynthetic processes, circadian rhythms, and responses to stimuli, most prominently light and radiation (Table S1, Figure 4D). Although leaves are the primary organs for photosynthesis, reproductive organs in many plant species are also photosynthetically active (Brazel and Ó'Maoiléidigh, 2019). The circadian control of photosynthesis in pistils might ensure the appropriate timing of carbon sources needed for reproductive success. Analyses of selected genes within these functional categories confirmed robust oscillations that were similar to the ones previously observed at the shoot apex (Figure 4E and Figure S4J-L). The rhythmic genes in pistils also included most of the morning- and evening-expressed core clock components (Figure 4F and Figure S4M-O). The waveforms oscillated with similar phases and amplitudes to those previously reported in whole seedlings or shoot apices (Takahashi et al., 2015) (Figure 4F-G). However, the evening-expressed core clock genes *TOC1* and *ELF3* showed weaker or no oscillation (Figure 4H and Figure S4P). Despite the weak rhythms, *TOC1* and *ELF3* have a relevant function within the pistil clock (see below), which suggest that translational and post-translational regulation might be important mechanisms for the circadian activity of the proteins.

To determine whether the circadian clock is indeed important for pistil function, we first used arrhythmic plants in which the clock is not able to properly run due to over-expression of *CCA1* (*CCA1-ox*). Our results showed that pistil length was significantly shorter in *CCA1-ox* compared to WT. The shorter pistil length was sustained at different pistil developmental stages (11, 12 and 13) (Müller, 1961; Smyth et al., 1990) (Figure 4I). The results suggest that proper circadian function is important for pistil growth, and that *CCA1* over-expression reduces the slope of pistil growth. To check whether changes in clock function also affect silique and seed production, we analyzed silique and seed number, length, weight and area. Our results showed that *CCA1-ox* produced less siliques that were significantly shorter than in WT (Figure 4J-K). The inspection of seeds in siliques also suggested developmental defects, with an increased number of abortive ovules in *CCA1-ox* (Figure

4L-M). Consistently, the number of seeds per silique, the seed mass and area were significantly reduced in *CCA1-ox* (Figure 4N-P).

To examine whether the effects were restricted to *CCA1-ox* or the circadian function is overall important for pistil growth and seed production, we examined mutant plants of different clock components in which the clock is still running although at a faster or slower pace than in WT. Our analyses showed that pistil length was also affected, particularly in double mutants, displaying reduced pistil size compared to that observed in WT (Figure 4Q). Mutation and over-expression of *TOC1* led to reduced and increased pistil length, respectively, and the phenotypes were sustained at different stages of pistil development (Figure 4R). *TOC1* miss-expressing plants also regulate hypocotyl length but show the reverse phenotypes, with *toc1-2* displaying long hypocotyls, and *TOC1-ox* showing longer than WT hypocotyl length (Mas et al., 2003a), which is in clear contrast with the pistil length phenotypes of *TOC1* miss-expressing plants. It is worth noting that the gradual increase in pistil length observed in the *prp* mutant plants correlated with a gradual increment in silique length and seed weight (Figure 4S-T). Altogether, the results indicate that proper function of the circadian clock is important for pistil and silique growth as well as for seed weight and production.

Transcriptional regulatory network at the core of the oscillator in pistils

To understand the circadian regulatory network in pistils, we examined gene expression in clock mutants and performed chromatin immunoprecipitation (ChIP) assays of key clock components. As in seedlings, the expression of *TOC1* and the *EC* genes was up-regulated in *cca1/lhy* double mutant (Figure 5A-C) suggesting that *CCA1* and *LHY* act as repressors of evening-expressed clock genes in pistils. The repression likely occurs through direct binding to the gene promoters as suggested by ChIP assays in pistils (Figure 5J). *cca1* and *lhy* double mutation also led to a marked down-regulation of *PRR7* and *PRR9* expression in pistils (Figure S5A-B). In turn, analyses of the *prp79* mutant showed an up-regulation of *CCA1* expression (Figure 5D) suggesting a direct repression of *CCA1* by *PRR9* and *PRR7*, as previously described in seedlings (Nakamichi, 2020). The evening-expressed genes were up-regulated during the subjective day but down-regulated during the subjective night in the *prp79* mutant (Figure S5C-F).

Mutation of the *EC* components *ELF3* and *LUX* resulted in increased expression of *PRR7* and *PRR9* (Figure 5E-F) and down-regulation of *CCA1* (Figure 5G). However, and contrarily to seedlings and roots, the mutation of *ELF4* did not lead to a relevant activation of *PRR9* expression (Figure 5E), which suggests that *ELF4* might not be part of the *EC* in the repression of *PRR9* or that an additional

function of ELF4 overcomes its EC-dependent regulation of *PRR9*. Consistent with the gene expression data, ChIP assays in pistils confirmed a significant binding of ELF3 and LUX to the promoters of the *PRR9* and *PRR7* genes, whereas ELF4 was not significantly enriched on these promoter regions (Figure 5K). Evening-expressed genes were up-regulated in the *ec* mutants (Figure S5G-J) as well as in the *toc1-2* mutant (Figure S5K). The *toc1-2* mutation also led to a reduced expression of *CCA1* and *LHY* (Figure 5H and Figure S5L) but an increased accumulation of *PRR7* (Figure 5I). Overall, we found that in the absence of functional *CCA1* and *LHY*, the morning-expressed *PRR* genes are repressed, whereas the evening-expressed genes are activated. On the other hand, mutation of evening-expressed genes results in down-regulation of *CCA1* and *LHY* and up-regulation of *PRR7*, *PRR9* and evening-expressed genes.

The data fit a model in which *CCA1* represses the expression of the evening-phased genes, and in turn these components repress *PRR9* and *PRR7*. *TOC1* also represses the expression of the *EC* genes, whereas *PRR9* and *PRR7* components repress *CCA1*. Analyses of mutants also provided interesting clues about the repressing functions. For instance, mutation of *CCA1* results in the marked down-regulation of *PRR9* and *PRR7* expression, which is likely the consequence of the up-regulation of the evening-phased repressor genes in the mutant. Similarly, the analyses of the *prr79* mutant suggest that *PRR9* and *PRR7* might repress (directly or indirectly) the evening-phased gene expression during the subjective day. The down-regulation of evening-phased gene expression during the subjective night might be a consequence of the up-regulation of *CCA1* in the *prr79* mutant. Similarly, by repressing *PRR9* and *PRR7* expression, the *EC* components up-regulate *CCA1* and *LHY* expression. Thus, the analyses of the mutants suggest that many of the clock components that function as repressors also shape the oscillations by repressing other repressors.

To identify canonical activators of clock gene expression in pistils, we examined the function of members of the REVEILLE (RVE) protein family, previously documented to be activators in whole seedlings (Ma et al., 2018; Rugnone et al., 2013; Xie et al., 2014). As previously described (Hsu et al., 2013), we found that in seedlings, the *rve4,6,8* triple mutant showed a clear phase-shift in the expression of oscillator genes (Figure 6A-C and Figure S6A-C). However, in pistils, the *rve4,6,8* triple mutant showed very weak amplitude or arrhythmia and resulted in a predominant down-regulation of *PRR5* and *TOC1* expression at nearly all time-points (Figure 6D-E). Notably, the expression of morning genes was also clearly affected with down-regulation during the subjective day and slight up-regulation during the subjective night (Figure 6F). Comparative analyses revealed the different effects of *rve4,6,8* triple mutant in seedlings versus pistils (Figure 6G-H and Figure S6D-

F). The different phenotypes were not due to the different nature of the two samples as mainly changes in amplitude were observed in comparisons of WT seedlings versus WT pistils (Figure S6G-I). The expression of *RVEs* was also reasonably similar in seedlings and pistils (Figure 6I), with *RVE6* showing low amplitude and *RVE8* displaying a phase-shift in pistils (Figure S6J-L). Together, the results suggest that in pistils, RVEs display a prevalent function controlling the expression of oscillator genes.

Genetic interaction studies on the repressive function of oscillator components

As the oscillator components regulate each other and share common targets, it is rather difficult to discern their specific function. To get insights into the morning and evening regulatory network, we performed genetic interaction studies and analyzed clock gene expression in pistils of *TOC1-ox/elf3-2* and in *CCA1-ox/prr79* plants. Studies with *TOC1-ox* pistils showed a highly repressing function of *TOC1-ox* (Figure 7A-D and Figure S7A-B). Comparative analyses using *TOC1-ox/elf3-2* pistils showed that over-expression of *TOC1* was able to overcome the up-regulation of the *PRR* genes in *elf3-2* mutants (Figure 7A-B and Figure S7B). Thus, *TOC1* repression of the *PRR* genes does not require a functional *ELF3*. A dominance of *TOC1-ox* repressive function on *PRRs* over the EC might explain these results. On the other hand, *ELF4* expression more closely resembled that observed in *elf3-2* mutant (see Figure S5H) than in *TOC1-ox* (Figure 7C), which suggests an *elf3-2* dominant phenotype, and a possible hierarchy of the EC auto-repression over the repressing function of *TOC1-ox*. It is also possible that *TOC1* requires *ELF3* for full repression of the EC. Similarly, *CCA1* gene expression was fully repressed in *TOC1-ox/elf3-2* resembling the phenotype observed in *elf3-2* mutant, although *CCA1* was still repressed in *TOC1-ox* (Figure 7D).

Analyses of *CCA1-ox* also showed a repressing function of *CCA1* that was not effectively overcome by the *prp79* mutation in the regulation of *TOC1* expression (Figure 7E). However, *ELF4* in *CCA1-ox/prp79* showed an up-regulation during the subjective day like the one observed in *prp79* mutant (Figure S5E) but not in *CCA1-ox* (Figure 7F). The results suggest that *CCA1* might require functional *PRR9* and *PRR7* for repression of *ELF4* or that the lack of the direct or indirect repressing function of *PRRs* can overcome the repression by *CCA1-ox*. Notably, analyses of *CCA1-ox/prp7* showed an evident up-regulation of *PRR9* expression (Figure S7E) suggesting that *PRR7* acts as a repressor of *PRR9* expression. Repression by *PRR7* is specific for *PRR9*, as *PRR5* expression was not up-regulated in *CCA1-ox/prp7* (Figure S7F). Analyses of clock gene expression in seedlings reinforced the differences on the regulation of the morning *PRRs* by the EC, particularly *PRR7* during the subjective night, and of *TOC1* and *ELF3* by the morning-expressed components during the subjective day

(compare Figure S7G-L with Figure 7B and E). Altogether, the analyses of mutants, over-expressing lines and the genetic interaction studies show a complex regulatory circuitry in pistils (Figure 7G) with CCA1-ox repressing *TOC1* over the morning PRRs (1); PRR7 repressing *PRR9* over CCA1-ox (2); morning PRRs repressing *CCA1* (3) and *EC* (4) over CCA1-ox. Within the evening-expressed components, *TOC1-ox* represses the *PRRs* over the *EC* (5), the *EC* auto-represses itself over *TOC1-ox* (6) and the *EC* activates *CCA1* over *TOC1-ox* (7).

DISCUSSION

Studies of the circadian regulatory networks in plants are increasingly shifting from whole seedlings to specific organs and tissues (Nakamichi, 2020; Sorkin and Nusinow, 2021). Key questions arise about the degree of circadian autonomy of tissues and organs, and the relevance of cell-to-cell coupling and long-distance circadian communication (Sorkin and Nusinow, 2021). Arabidopsis tissues with high cell density such as those at the shoot and root meristems favor circadian coupling (Sorkin and Nusinow, 2021). Consistently, the shoot apex and the tip of the root clocks have been proposed as coordinating signaling nodes influencing rhythms in other parts of the plant (Gould et al., 2018; Takahashi et al., 2015). Overall, the results thus far fit the notion of tissue-specific clocks that also require cell-to-cell and long distance coordination for circadian precision and responses to environmental cues (Nakamichi, 2020; Sorkin and Nusinow, 2021). To fully understand the circadian function and communication, it is important to elucidate the similarities and differences of the circadian regulatory network in cells, tissues and organs.

Our studies have shown that buds and flowers detached from the rest of the plant display rhythmic oscillations, which indicate the presence of self-sustained functional clocks. The developmental differences (e.g. in buds and open flowers) may be due to different sensitivities to environmental cues (Atamian et al., 2016). Under our conditions, other excised organs, for example roots, also sustain rhythms but with a long period and delayed phase compared to shoots (Chen et al., 2020; Takahashi et al., 2015). Notably, excised pistils showed self-sustained rhythms with precise 24-h oscillations. These results indicate the presence of a clock that is able to precisely run even in the absence of signals from the rest of the plant. In other floral organs, the dampened rhythms could be due to reduced viability or lack of energy after excision from the flower. Future studies should focus on understanding the circadian regulatory network in sepals, petals and stamens as well as on their circadian robustness after several days under LL. Compared to pistils, rhythms in stamens displayed a short period phenotype. It would be interesting to determine the biological relevance of such

variation between the reproductive organs. Circadian differences in reproductive organs are not exclusive of plants. For instance, the expression of core clock genes is also rhythmic in ovarian tissues (Kennaway et al., 2012), and female and male rats show sex differences in daily rhythms and in responses to endogenous and exogenous cues (Bailey and Silver, 2014). The sex-dependent circadian differences are relevant to humans in many areas, most notably those related to reproduction and overall health (Bailey and Silver, 2014). Understanding the circadian clockwork in flowers may prove essential for optimizing plant reproduction and productivity.

Clock repressors and activators have specific regulatory functions in pistils. For instance, RVE proteins appear to have a prevalent activating function in pistils. The low amplitude or arrhythmic phenotypes of the *rve4,6,8* triple mutant in pistils are in sharp contrast with the clear oscillations observed in seedlings. In sepals, petals and stamens, the *toc1-2* mutant showed similar waveforms than WT at least for the first days under LL. These results suggest that the lack of a functional TOC1 can be overcome for few days. In pistils, on the other hand, the short period phenotype is evident from the initial days but the rhythms dampened low over time. Thus, TOC1 circadian function is different in the floral organs, with a prevalent role in pistils. The expression of oscillator genes in pistils is similar to the one previously described with some exceptions like *ELF3*. Translational and/or post-translational mechanisms of regulation might contribute to the rhythmic oscillation of clock protein activity. For example, TOC1 protein is regulated by degradation through the proteasome pathway thus providing a mechanism for controlling TOC1 protein oscillation and period length by the clock (Mas et al., 2003b).

Genome-wide analyses of the circadian transcriptional landscape in pistils showed the importance of the circadian clock regulating photosynthesis and responses to environmental signals. Photosynthesis is not exclusive of leaves as it is also present in reproductive organs (Brazel and Ó'Maoiléidigh, 2019). It has been suggested that photosynthesis in reproductive organs may represent an adaptive trait, not only by balancing the carbon cost of reproduction but also conferring resistance to abiotic stresses (Raven and Griffiths, 2015). Some possible disadvantages of the photosynthetic activity include the increased DNA damage and the production of reactive oxygen species. Thus, proper timing of photosynthesis in pistils by the circadian clock might be beneficial for ensuring enough energy resources when needed but may also activate responses to cope with DNA damage. Consistently, the circadian clock in pistils coordinates responses to radiation, light, and abiotic stimulus. In humans and animal models, increasing evidence is pointing out relevant processes controlled by the clock that show sex differences in daily rhythms including, among others, the sleep-

wake cycle, hormonal and metabolic oscillations (Mong et al., 2011). Proper circadian function is also important for pistil and silique growth as well as for seed quality and production. It would be interesting to determine the molecular mechanisms and downstream signaling pathways by which the circadian clock regulates pistil growth and function. The circadian factors and regulatory mechanisms controlling growth appear to be organ-specific, judging by the opposite hypocotyl and pistil length phenotypes observed in plants miss-expressing clock components. The circadian clock implication in the control of seed production opens interesting possibilities for biotechnological application of improving seed yield, arguably one of the most important traits for plant breeding.

Analyses of mutant and over-expressing lines point out to a complex regulatory network for the pistil clock. The transcriptional regulatory activity does not sustain robust amplitude of *TOC1* and *ELF3* mRNA expression in pistils as opposed to their rhythms observed in seedlings. Furthermore, the specific phenotypes of *toc1-2*, the different behavior of the *ec* mutants regulating *PRR9* and *PRR7* circadian expression, and the clock gene expression patterns in *rve* mutant, all indicate some specificities of the pistil clock. The changes were also confirmed in the seedling analyses of the clock over-expressing/mutant lines. The genetic interaction studies also suggest dominant repressive phenotypes, able to overcome either the over-expression or the mutation of other oscillator components. Current models of the Arabidopsis clock in whole seedlings include the reciprocal regulation of morning and evening oscillator genes that results in their time-of-day specific peak of expression (Avello et al., 2021). Other models also group several circadian components together (Avello et al., 2021; Caluwé et al., 2016). The particular circadian architecture that we found in pistils might provide robustness to the pistil clockwork. Our results pave the way for a better understanding of the circadian system in the reproductive organs, which might likely provide biotechnological tools to manipulate plant reproduction and hence productivity.

Limitations of the study

In this study, we have focused on the transcriptional regulatory network at the core of the pistil clock. However, we have not elucidated the network in other floral organs including sepals, petals and stamens. Floral organs other than pistils are short-lived in planta so that reduced viability and/or the lack of energy after excision might contribute to the dampening of the rhythms that we observed in the bioluminescence assays. We propose that detailed time course analyses by RT-QPCR will provide useful information about the circadian networks in other floral organs. We have also not provided evidence of the biological relevance of the different circadian periods observed in pistils and stamens. Likewise, we have not identified the molecular mechanisms responsible for the circadian control of

pistil growth. These interesting aspects are important to fully understand the flower clock in *Arabidopsis*.

ACKNOWLEDGMENTS

We thank Prof. Wu (Academia Sinica, Taipei, Taiwan) for the *GI::LUC* seeds, and Lu Xiong (CRAG, Spain) for help with the pictures. The Mas laboratory is funded with a Research Grant (PID2019-106653GB-I00) from MCIN/ AEI/10.13039/501100011033, from the Ramon Areces Foundation, and from the Generalitat de Catalunya (AGAUR) (2017 SGR 1211). PM laboratory also acknowledges financial support from the CERCA Program/Generalitat de Catalunya and by the Spanish Ministry of Economy and Competitiveness through the “Severo Ochoa Program for Centers of Excellence in R&D” (CEX2019-000902-S) funded by MCIN/ AEI/10.13039/501100011033. MO was a recipient of a “Severo Ochoa” Internationalization Postdoctoral Program fellowship. Z.Y.Y. is a recipient of a Chinese Scholarship Council (CSC) fellowship.

AUTHOR CONTRIBUTIONS

MO and ZY performed the experiments. PM conceived the project, designed the experiments, and wrote the manuscript. All authors read, revised, and approved the manuscript.

DECLARATION OF INTEREST

The authors declare no competing interests.

INCLUSION AND DIVERSITY

We support inclusive, diverse, and equitable conduct of research.

FIGURE LEGENDS

Figure 1. Self-sustained circadian rhythms in buds and flowers. (A) Representative photographs of buds and flowers at different developmental stages. In vivo luminescence assays of *CCA1::LUC* rhythms in (B) young and mature buds and (D) young and mature flowers. Period, and relative amplitude error estimates of circadian rhythms of (C) young and mature buds and (E) mature and open flowers. Circadian time course analyses by RT-QPCR of (F) *CCA1* and (G) *ELF4* mRNA expression in open flowers. Samples were examined under constant light (LL) following synchronization under light:dark cycles (16h light:8h dark). Data are presented as the mean +SEM.

Scale bar = 1 mm. At least two biological replicates were performed per experiment. See also Figure S1.

Figure 2. Distinct phenotypes of *toc1-2* mutant in buds and in flowers. In vivo luminescence assays of *CCA1:LUC* rhythms in WT and *toc1-2* (A) young buds, (B) open flowers, (C) mature buds and (D) mature flowers. Period, and relative amplitude error estimates of *CCA1:LUC* rhythms in WT and *toc1-2* (E) mature buds and (F) open flowers. (G) Comparative luminescence analyses of *CCA1:LUC* rhythms in WT and *toc1-2* mature buds and open flowers. (H) Period, and relative amplitude error estimates of *CCA1:LUC* rhythms in *toc1-2* mature buds and open flowers. Samples were examined under LL following synchronization under light:dark cycles (16h light:8h dark). Data are presented as the mean +SEM. At least two biological replicates were performed per experiment. Data are repeated in different graphs to facilitate comparisons.

Figure 3. Robust circadian oscillations in pistils require a functional TOC1. (A) Representative photographs of sepals, petals, stamens and pistils. (B) In vivo luminescence assays of *CCA1:LUC* rhythms in WT and *toc1-2* (B) sepals, (C) petals, (D) stamens and (E) pistils. Comparative waveform analyses of *CCA1:LUC* rhythms in WT (F) petals and pistils and (G) stamens and pistils. Period, and relative amplitude error estimates of circadian rhythms in WT (H) sepals and pistils, (I) stamens and sepals, and (J) stamens and pistils. Samples were examined under LL following synchronization under light:dark cycles (16h light:8h dark). Data is presented as mean +SEM. At least two biological replicates were performed per experiment. Data are repeated in different graphs to facilitate comparisons among floral organs. Scale bar = 0.5 mm. See also Figure S2 and S3.

Figure 4. Circadian transcriptional landscape in pistils and regulation of pistil growth and seed production. (A) Expression-based heatmap from transcriptomic RNA-Seq data at different circadian times. (B) Relative amplitude and (C) phase estimates of oscillating genes in pistils. (D) Functional categorization of the main circadian genes in pistils. (E) Comparative time course analysis of *PIL6* gene expression from RNA-Seq data in pistils and shoot apex. (F) Expression-based heatmap from RNA-Seq data of the main oscillator genes at different circadian times. Comparative time course analysis of *CCA1* and *TOC1* gene-expression from RNA-Seq data in (G) shoot apex and (H) pistils. Analyses of (I) pistil length, (J) silique number, and (K) silique length in WT and *CCA1-ox* plants. Representative images of seeds in siliques of (L) WT and (M) *CCA1-ox* plants. Siliques are not displayed in full length to facilitate the visualization of the seeds. Analyses of (N) seed number per silique, (O) seed weight, and (P) seed sectional area in WT and *CCA1-ox* plants. Analyses of pistil

length in (Q) the *prp* mutants and (R) *toc1-2* and TOC1-ox plants. Analyses of (S) silique length and (T) seed weight in the *prp* mutants. Data is presented as mean \pm SEM. (***) p-value<0.0001; ** p-value>0.001; * p-value<0.05). Scale bar = 0.5 mm. See also Figure S4.

Figure 5. Regulatory network at the core of the pistil oscillator in clock mutants. Time course analysis by RT-QPCR of (A) *TOC1*, (B) *ELF4* and (C) *LUX* gene expression in WT and *cca1-1llhy-RNAi* pistils. (D) *CCA1* gene expression in WT and *prp79* mutant pistils. (E) *PRR9*, (F) *PRR7* and (G) *CCA1* gene expression in WT and *elf3-2*, *lux-2* and *elf4-2* pistils. (H) *CCA1*, and (I) *PRR7* in WT and *toc1-2* pistils. ChIP analyses of (J) *CCA1* at ZT3, (K) *ELF3*, and *ELF4* at ZT15, and (L) *LUX* and *ELF4* at ZT15 showing the enrichment (relative to the input) to the target promoters. Data are presented as the mean +SEM. For comparative analyses ChIP assays of *ELF4* are shown in K and L. At least two biological replicates were performed per experiment. See also Figure S5.

Figure 6. Distinct regulatory role of RVEs at the core of the pistil oscillator. Comparative time course analysis by RT-QPCR in WT and *rve4,6,8* seedlings (A-C) and WT and *rve4,6,8* pistils (D-F). (A, D) *PRR5* gene expression. (B, E, G) *TOC1* gene expression. (C, F, H) *PRR9* gene expression. Comparison of (G) *TOC1* (H) *PRR9* gene expression in *rve4,6,8* seedlings and *rve4,6,8* pistils. (I) Comparison of *RVE4* expression in seedlings and pistils. Data are repeated in different graphs to facilitate comparisons. (I) Data are presented as the mean +SEM. Two biological replicates were performed for the analyses in seedlings, whereas three biological replicates were performed for the analyses in pistils. See also Figure S6.

Figure 7. Genetic interaction analyses of the transcriptional repressive networks at the core of the pistil oscillator. Time course analysis by RT-QPCR of (A) *PRR9*, (B) *PRR7*, (C) *ELF4*, and (D) *CCA1* gene expression in WT, TOC1-ox and TOC1-ox/*elf3-2* pistils. (E) *TOC1* and (F) *ELF4* gene expression in WT and *CCA1-ox/prp79* pistils. Data are presented as the mean +SEM. Three biological replicates were performed per experiment. (G) Circadian regulatory network comprising dominant regulatory functions (thick black lines) as inferred by the genetic interaction studies. See the main text for a further explanation. See also Figure S7.

STAR Methods

RESOURCE AVAILABILITY

Lead contact

Further information and requests for resources and reagents should be directed to and will be fulfilled by the lead contact, Paloma Mas (paloma.mas@cragenomica.es).

Materials availability

All materials generated in this study will be available upon request from Paloma Mas (paloma.mas@cragenomica.es).

Data and code availability

- The RNA-sequencing data have been deposited at the Sequence Read Archive and are publicly available as of the date of publication. Accession number is listed in the key resources table.
- This paper does not report original code.
- Any additional information required to reanalyze the data reported in this paper is available from the lead contact upon request.

EXPERIMENTAL MODEL AND SUBJECT DETAILS

Plant material, growing conditions and organ dissection

Seedlings were grown on half-strength Murashige and Skoog (MS) agar medium without sucrose, and synchronized under light:dark cycles (LgD, 16h light:8h dark) with 60-100 $\mu\text{mol m}^{-2}\text{s}^{-1}$ of cool white fluorescent light at 22°C for about 7-10 days (unless otherwise specified). For experiments using flowering plants, seedlings were then transplanted to soil and cultivated throughout the reproductive stage under light:dark cycles (LgD, 16h light:8h dark) with 150-200 $\mu\text{mol m}^{-2}\text{s}^{-1}$ of white light emitting diodes (LEDs) at 22°C. The *CCA1:LUC* (Salomé and McClung, 2005), *TOC1:LUC* (Perales and Más, 2007) and *GI:LUC* (Wu et al., 2008) reporter lines as well as the *CCA1-ox* (Wang and Tobin, 1998), *TOC1-ox* (Huang et al., 2012), and *toc1-2;CCA1:LUC* (NASC, N2107710) (Cervela-Cardona et al., 2021), *cca1-1/lhy-RNAi* (Alabadí et al., 2002), *lux-2* (Hazen et al., 2005), *elf3-2* (Hicks et al., 1996), *elf4-2* (Huang et al., 2016), *prr5-11;CCA1:LUC*, *prr57*, *prr59* (Nakamichi et al., 2005), *prr79* (Farré et al., 2005), *rve4,6,8* (Hsu et al., 2013), *ELF3-ox-YFP* (Herrero et al., 2012), *YFP-ELF4-ox* (Herrero et al., 2012), *LUX-GFP* (*LUXpro::LUX-GFP lux-4*) (Ezer et al., 2017), *CCA1-HA-EYFP/cca1-1* (Yakir et al., 2009) lines were described elsewhere. All the lines are in Columbia (Col-0) background except the *cca1-1/lhy-RNAi* plants, which are in Wassilewskija (WS) background. Matching WT backgrounds were used for each mutant line. The *TOC1-ox/elf3-2* lines were generated by crossing the *TOC1-ox* plants (Huang et al., 2012) with the

elf3-2 mutant (Hicks et al., 1996). The CCA1-ox/*prp* lines were generated by transforming the CCA1-ox construct into the *prp79* plants and by crossing the CCA1-ox plants (Wang and Tobin, 1998) with the *prp7* mutant plants (Farré et al., 2005). To follow individual open flowers in intact plants, inflorescences of open flowers were marked by a black marker at day 0 under LL. Pictures of the selected flowers were taken with a stereo microscope (SZX16, Olympus) the following days. For the luminescence assays (see below) and for the RT-QPCR (Reverse Transcription Quantitative Polymerase Chain Reaction) analysis of floral organs, sterile dissecting forceps were used to carefully excise young buds, mature buds, mature flowers and open flowers from flowering plants. Similarly, sepals, petals, stamens, and pistils were carefully excised from open flowers.

METHODS DETAILS

In vivo luminescence assays

Buds, flowers or floral organs from luciferase-expressing plants synchronized under light:dark cycles (LgD, 16h light:8h dark) with 150-200 $\mu\text{mol m}^{-2}\text{s}^{-1}$ of white LEDs at 22°C were excised and immediately placed in 96-well microplates with half-strength MS liquid medium with 1% sucrose and 290 μM D-luciferin (Biothema). Bioluminescence rhythms, were examined as previously described (Okada and Mas, 2022) under constant light (LL) conditions or entraining Light:Dark cycles (LgD, 16h light:8h dark) as specified for each experiment. A microplate luminometer LB-960 (Berthold Technologies) and the software Microwin, version 4.34 (Mikrotek 2 Laborsysteme) were used for the bioluminescence analyses. Amplitude, period, and relative amplitude error (RAE) were estimated with the fast Fourier transform non-linear least squares (FFT-NLLS) method (Zielinski et al., 2014). The analyses were performed in the statistical environment of R 3.3.2. Data from samples that appeared damaged or that eventually died in the wells were excluded from the analyses. Three biological replicates were performed per experiment.

Gene expression analysis by RT-QPCR

About 5-6 12-day old seedlings or about 6-8 flowers were collected, snap-frozen and ground using TissueLyser II (QIAGEN). About 6-8 pistils were collected, snap-frozen and ground using plastic grinding pestles. About 70 stamens were collected in homogenization solution (Promega, Z305H), snap-frozen, and ground using plastic grinding pestles. RNA from flowers, stamens and pistils was isolated using the Maxwell RSC Plant RNA kit (Promega). Single strand cDNA was synthesized using iScript™ Reverse Transcription Supermix for RT-qPCR (BioRad) following the manufacturer recommendations. For QPCR analysis, cDNAs were diluted 30-50-fold with nuclease-free water and QPCR was performed with Brilliant III ultrafast SYBR qRT-PCR Master Mix (Agilent) in a 96-well

CFX96 Touch Real-Time PCR Detection System (BioRad). The *IPP2* gene (Fung-Uceda et al., 2018) was used as control in seedlings and *PP2AA3* (AT1G13320) (Takahashi et al., 2015) was used as control in pistil and flowers. A list of primers used for gene expression analyses is shown in Supplemental Table 2.

RNA-Seq analysis

Plants were synchronized under LgD conditions (16h light:8h dark) with 150-200 $\mu\text{mol m}^{-2}\text{s}^{-1}$ of white LEDs at 22°C and subsequently transferred to LL for two days. About 6-8 pistils from open flowers were collected the third day under LL, every four hours over two circadian cycles. Total RNA was isolated using the Maxwell RSC Plant RNA kit (Promega) following the manufacturer's recommendations. Sequencing was performed by Novogene Co., Ltd. RNA purity was checked using a NanoPhotometer® spectrophotometer (IMPLEN, CA, USA) and RNA integrity and quantitation were assessed using the RNA Nano 6000 Assay Kit of the Bioanalyzer 2100 system (Agilent Technologies). A total of 1 μg RNA per sample was used for the RNA sample preparations. Sequencing libraries were generated using NEBNext® Ultra™ RNA Library Prep Kit for Illumina® (NEB) following manufacturer's recommendations. Index codes were added to attribute sequences to each sample. mRNA was purified from total RNA using poly-T oligo-attached magnetic beads. Fragmentation was carried out using divalent cations under elevated temperature in NEBNext First Strand Synthesis Reaction Buffer (5X). First strand cDNA was synthesized using random hexamer primer and M-MuLV Reverse Transcriptase (RNase H). Second strand cDNA synthesis was subsequently performed using DNA Polymerase I and RNase H. Remaining overhangs were converted into blunt ends via exonuclease/polymerase activities. After adenylation of 3' ends of DNA fragments, NEBNext Adaptor with hairpin loop structure were ligated to prepare for hybridization. In order to select cDNA fragments of preferentially 150~200 bp in length, the library fragments were purified with AMPure XP system (Beckman Coulter). Subsequently, 3 μl of USER Enzyme (NEB) were used with size-selected, adaptor ligated cDNA at 37 °C for 15 min followed by 5 min at 95 °C before PCR. PCR was performed with Phusion High-Fidelity DNA polymerase, Universal PCR primers and Index (X) Primer. The PCR products were purified (AMPure XP system) and library quality was assessed on the Agilent Bioanalyzer 2100 system.

Clustering of the index-coded samples was performed on a cBot Cluster Generation System using PE Cluster Kit cBot-HS (Illumina) according to the manufacturer's instructions. After clustering, the library preparations were sequenced on an Illumina platform and paired-end reads were generated. Raw data (raw reads) of FASTQ format were firstly processed through fastp. In this step, clean data

(clean reads) were obtained by removing reads containing adapter and poly-N sequences and reads with low quality from raw data. At the same time, Q20, Q30 and GC content of the clean data were calculated. All the downstream analyses were based on the clean data with high quality. Paired-end clean reads were mapped to the reference genome using HISAT2 software (Kim et al., 2019). HISAT2 uses a large set of small GFM indexes that collectively cover the whole genome. These small indexes (called local indexes), combined with several alignment strategies, enable rapid and accurate alignment of sequencing reads. Featurecounts was used to count the read numbers mapped of each gene. RPKM (Reads Per Kilobase of exon model per Million mapped reads) of each gene was calculated based on the length of the gene and reads count mapped to this gene. RPKM considers the effect of sequencing depth and gene length for the reads count at the same time and is currently the most commonly used method for estimating gene expression levels. The web-based tool “Heatmapper” was used to visualize data as heatmaps (Babicki et al., 2016).

The JTK_Cycle algorithm (Hughes et al., 2010) was used to identify oscillating genes (adjusted p-value < 0.05) with a period ranging from 20 to 28. The Integrative Genomics Viewer (IGV) was used to visualize the data (Robinson et al., 2011; Thorvaldsdóttir et al., 2013). The phases of circadian expression were analyzed using the publicly available Gene Phase Analysis Tool “PHASER” of the DIURNAL database (<http://diurnal.mocklerlab.org/>) (Michael et al., 2008; Mockler et al., 2007). Phase over-representation is calculated as the number of genes with a given phase divided by the total number of genes over the number of genes called rhythmic and divided by the total number of genes in the dataset. Circadian genes were classified into broad functional categories using the PANTHER Over-representation Test (Fisher’s Exact Test, Bonferroni correction) and the web tool “BIOMAPS” (Katari et al., 2010) (Fisher’s Exact Test, cut-off 0.01), which renders over-represented and significant functional terms (Gene Ontology or MIPS) as compared to the frequency of the term in the whole genome.

Phenotypic analyses of pistils, siliques and seeds

For pistil analyses, at least 5 pistils for each genotype were selected at stages 11, 12 and 13 (Müller, 1961; Smyth et al., 1990), and pictures were taken with a stereo microscope (SZX16, Olympus) after careful removal of petals and sepals. Measurements of pistil length was performed by using the software package *Image J*. For silique and seed analyses, 100 fully developed siliques from the main inflorescences (starting at the fifth silique from the bottom) were collected and photographed using a stereo microscope (SZX16, Olympus). Seeds from each silique were spread on white paper and photographs were taken. Silique length and seed number per silique were quantified using the

software package *Image J*. For seed size and weight analyses, seeds were harvested and sieved to remove plant debris. Following incubation at 25°C for 7 days, randomly selected groups of seeds for each line were weighted (W). Seed number (N), sectional area, length and width were quantified using the software package *Image J*. The grain weight was calculated as: $1000\text{-grain weight (g)} = W / N * 1000$. Two-tailed Student's *t*-test analyses were performed using the GraphPad Prism software.

Chromatin immunoprecipitation assays

Chromatin immunoprecipitation (ChIP) assays were performed as previously described (Yamaguchi et al., 2014). About 100 mg of pistils from open flowers were sampled, and vacuum infiltrated 3 times for 15 min in 30 ml cross-linking solution (1% formaldehyde in 1×PBS) at room temperature. The cross-linking reaction was stopped by adding glycine to a final concentration of 0.125 M and vacuum infiltrated for 5 min. Samples were washed three times with cold deionized water, dried with paper towels and snapped-frozen in liquid nitrogen. Samples were ground to fine powder and extracted with 2.5 ml of Nuclei extraction buffer. After filtering the samples through Miracloth (475855, Merck), the chromatin solution was sonicated until obtaining sheared DNA of about 200-600 bp. Soluble chromatin was incubated overnight at 4°C with the Anti-GFP antibody (#A-11122, Thermo Fisher Scientific) for the samples of ELF3-ox-YFP, YFP-ox-ELF4, LUX-GFP and CCA1-HA-EYFP/*cca1-1*. Samples were then incubated with Protein G-Dynabeads beads (10004D, Thermo Fisher Scientific) for 4 hours at 4°C with rotation. The beads were washed thrice with Low salt wash buffer, High salt wash buffer, 250 mM LiCl wash buffer and 0.5×TE, respectively. The samples were eluted from the beads with elution buffer by incubating for 30 min at 65°C. The purified DNA was diluted 10-fold with nuclease-free water and QPCR was performed with Brilliant III ultrafast SYBR qRT-PCR Master Mix (Agilent) in a 96-well CFX96 Touch Real-Time PCR Detection System (BioRad). A list of primers used for ChIP analyses is shown in Supplemental Table S2.

QUANTIFICATION AND STATISTICAL ANALYSIS

For luminescence assays, data represent means + SEM of $n \geq 3$ (Figures 1B, 1D, S1, 2A-2D, 2G, S2A-S2F, 3B-3G, S3E-S3F). Periods and relative amplitude errors of bioluminescence rhythms were estimated with the fast Fourier transform non-linear least squares (FFT-NLLS) and plotted with three biological replicates (Figures 1C, 1E, 2E-2F, 2H, 3H-3J, S3A-S3D). Statistical analyses were performed by two-tailed Student's *t*-test to compare period lengths. Quantification of pistil length (Figures 4I, 4Q, and 4R), silique length (Figures 4K and 4S), seed number (Figure 4N), and seed sectional area (Figure 4P) was performed using ImageJ software. For pistil length, data represent median ± SEM of $n \approx 15$ pistils (Figures 4I, 4Q, and 4R). For silique number, data represent median

\pm SEM of $n \approx 15$ plants (Figure 4J). For silique length, $n \approx 100$ siliques were measured. Data represent median \pm SEM (Figure 4K), lengths are plotted with the means (Figure 4S). For seed number per silique, data represent median \pm SEM of $n \approx 70$ siliques (Figure 4N). For 1000-grain-weight, more than 500 seeds were weighed, and data represent median \pm SEM of $n \approx 12$ (Figure 4O). For seed sectional area, areas of $n \approx 200$ seeds are plotted with those means (Figure 4P). For seed weights per plants, $n \approx 30$ plants were used and weights of seeds from each plant are plotted with those means (Figure 4T). Statistical analyses were performed by two-tailed Student's *t*-test (***p*-value <0.0001 ; ***p*-value >0.001 ; **p*-value <0.05). For gene expression analysis using qPCR (Figures 1F-1G, S2G-S2H, S2J-S2M, 5, S5, 6, S6, 7A-7F, S7), data represent means \pm SEM of technical duplicates using three biological replicates. Crossing point (Cp) calculation was used for quantification using the Absolute Quantification analysis by the 2nd Derivative Maximum method.

Supplemental Table S1. JTK_CYCLE analysis and biological process enrichment of rhythmic genes in pistils. Related to Figure 4.

REFERENCES

REFERENCES

- Adams, S., and Carré, I.A. (2011). Downstream of the plant circadian clock: output pathways for the control of physiology and development. *Essays Biochem.* *49*, 53–69. <https://doi.org/10.1042/bse0490053>.
- Alabadí, D., Yanovsky, M.J., Más, P., Harmer, S.L., Kay, S.A. (2002). Critical role for CCA1 and LHY in maintaining circadian rhythmicity in *Arabidopsis*. *Curr Biol* *12*, 757–761. [https://doi.org/10.1016/S0960-9822\(02\)00815-1](https://doi.org/10.1016/S0960-9822(02)00815-1).
- Atamian, H.S., Creux, N.M., Brown, E.A., Garner, A.G., Blackman, B.K., and Harmer, S.L. (2016). Circadian regulation of sunflower heliotropism, floral orientation, and pollinator visits. *Science* *353*, 587–590. <https://doi.org/10.1126/science.aaf9793>.
- Atkins, K.A., and Dodd, A.N. (2014). Circadian regulation of chloroplasts. *Curr. Opin. Plant Biol.* *21*, 43–50. <https://doi.org/10.1016/j.pbi.2014.06.008>.
- Avello, P.A., Davis, S.J., and Pitchford, J. (2021). Temperature robustness in *Arabidopsis* circadian clock models is facilitated by repressive interactions, autoregulation, and three-node feedbacks. *J. Theor. Biol.* *509*. <https://doi.org/10.1016/J.JTBI.2020.110495>.
- Babicki, S., Arndt, D., Marcu, A., Liang, Y., Grant, J.R., Maciejewski, A., and Wishart, D.S. (2016). Heatmapper: web-enabled heat mapping for all. *Nucleic Acids Res.* *44*, W147–W153. <https://doi.org/10.1093/nar/gkw419>.

- Bailey, M., and Silver, R. (2014). Sex differences in circadian timing systems: implications for disease. *Front. Neuroendocrinol.* *35*, 111–139. <https://doi.org/10.1016/J.YFRNE.2013.11.003>.
- Bordage, S., Sullivan, S., Laird, J., Millar, A.J., and Nimmo, H.G. (2016). Organ specificity in the plant circadian system is explained by different light inputs to the shoot and root clocks. *New Phytol.* *212*, 136–149. <https://doi.org/10.1111/nph.14024>.
- Brazel, A.J., and Ó'Maoiléidigh, D.S. (2019). Photosynthetic activity of reproductive organs. *J. Exp. Bot.* *70*, 1737–1754. <https://doi.org/10.1093/JXB/ERZ033>.
- Caluwé, J. De, Xiao, Q., Hermans, C., Verbruggen, N., Leloup, J.-C., and Gonze, D. (2016). A Compact Model for the Complex Plant Circadian Clock. *Front. Plant Sci.* *7*, 74. <https://doi.org/10.3389/FPLS.2016.00074>.
- Cervela-Cardona, L., Yoshida, T., Zhang, Y., Okada, M., Fernie, A., and Mas, P. (2021). Circadian Control of Metabolism by the Clock Component TOC1. *Front. Plant Sci.* *12*, 1126. <https://doi.org/10.3389/fpls.2021.683516>.
- Chen, Z.J., and Mas, P. (2019). Interactive roles of chromatin regulation and circadian clock function in plants. *Genome Biol.* *20*, 1-12. <https://doi.org/10.1186/s13059-019-1672-9>.
- Chen, W.W., Takahashi, N., Hirata, Y., Ronald, J., Porco, S., Davis, S.J., Nusinow, D.A., Kay, S.A., and Mas, P. (2020). A mobile ELF4 delivers circadian temperature information from shoots to roots. *Nat. Plants* *6*, 416–426. <https://doi.org/10.1038/s41477-020-0634-2>.
- Creux, N.M., Brown, E.A., Garner, A.G., Saeed, S., Scher, C.L., Holalu, S. V., Yang, D., Maloof, J.N., Blackman, B.K., and Harmer, S.L. (2021). Flower orientation influences floral temperature, pollinator visits, and plant fitness. *New Phytol.* *232*, 868-879. <https://doi.org/10.1111/nph.17627>.
- Crosby, P., and Partch, C.L. (2020). New insights into non-transcriptional regulation of mammalian core clock proteins. *J. Cell Sci.* *133*, jcs241174. <https://doi.org/10.1242/jcs.241174>.
- Drews, G.N., Weigel, D., and Meyerowitz, E.M. (1991). Floral patterning. *Curr. Opin. Genet. Dev.* *1*, 174–178. [https://doi.org/10.1016/S0959-437X\(05\)80066-8](https://doi.org/10.1016/S0959-437X(05)80066-8).
- Endo, M., Shimizu, H., Nohales, M.A., Araki, T., and Kay, S.A. (2014). Tissue-specific clocks in *Arabidopsis* show asymmetric coupling. *Nature* *515*, 419–422. <https://doi.org/10.1038/nature13919>.
- Ezer, D., Jung, J.H., Lan, H., Biswas, S., Gregoire, L., Box, M.S., Charoensawan, V., Cortijo, S., Lai, X., Stöckle, D., et al. (2017). The evening complex coordinates environmental and endogenous signals in *Arabidopsis*. *Nat. Plants* *3*, 1-12. <https://doi.org/10.1038/nplants.2017.87>.
- Farinas, B., and Mas, P. (2011). Functional implication of the MYB transcription factor RVE8/LCL5 in the circadian control of histone acetylation. *Plant J.* *66*, 318-329. <https://doi.org/10.1111/j.1365-313X.2011.04484.x>.
- Farré, E.M., Harmer, S.L., Harmon, F.G., Yanovsky, M.J., and Kay, S.A. (2005). Overlapping and

distinct roles of PRR7 and PRR9 in the Arabidopsis circadian clock. *Curr. Biol.* *15*, 47–54. <https://doi.org/10.1016/j.cub.2004.12.067>.

Fenske, M.P., and Imaizumi, T. (2016). Circadian rhythms in floral scent emission. *Front. Plant Sci.* *7*, 462. <https://doi.org/10.3389/fpls.2016.00462>.

Fenske, M.P., Nguyen, L.A.P., Horn, E.K., Riffell, J.A., and Imaizumi, T. (2018). Circadian clocks of both plants and pollinators influence flower seeking behavior of the pollinator hawkmoth *Manduca sexta*. *Sci. Rep.* *8*, 1-13. <https://doi.org/10.1038/s41598-018-21251-x>.

Ferrándiz, C., Pelaz, S., and Yanofsky, M.F. (1999). Control of carpel and fruit development in Arabidopsis. *Annu. Rev. Biochem.* *68*, 321–354. <https://doi.org/10.1146/annurev.biochem.68.1.321>.

Flis, A., Mengin, V., Ivakov, A.A., Mugford, S.T., Hubberten, H.M., Encke, B., Krohn, N., Höhne, M., Feil, R., Hoefgen, R., et al. (2019). Multiple circadian clock outputs regulate diel turnover of carbon and nitrogen reserves. *Plant Cell Environ.* *42*, 549–573. <https://doi.org/10.1111/pce.13440>.

Fukuda, H., Nakamichi, N., Hisatsune, M., Murase, H., and Mizuno, T. (2007). Synchronization of plant circadian oscillators with a phase delay effect of the vein network. *Phys. Rev. Lett.* *99*, 098102. <https://doi.org/10.1103/PhysRevLett.99.098102>.

Fukuda, H., Ukai, K., and Oyama, T. (2012). Self-arrangement of cellular circadian rhythms through phase-resetting in plant roots. *Phys. Rev. E.* *86*, 041917. <https://doi.org/10.1103/PhysRevE.86.041917>.

Fukushima, A., Kusano, M., Nakamichi, N., Kobayashi, M., Hayashi, N., Sakakibara, H., Mizuno, T., and Saito, K. (2009). Impact of clock-associated Arabidopsis pseudoresponse regulators in metabolic coordination. *Proc. Natl. Acad. Sci. U.S.A.* *106*, 7251–7256. <https://doi.org/10.1073/pnas.0900952106>.

Fung-Uceda, J., Lee, K., Seo, P.J.P.J., Polyn, S., De Veylder, L., and Mas, P. (2018). The Circadian Clock Sets the Time of DNA Replication Licensing to Regulate Growth in Arabidopsis. *Dev. Cell* *45*, 101-113. <https://doi.org/10.1016/j.devcel.2018.02.022>.

Gould, P.D., Domijan, M., Greenwood, M., Tokuda, I.T., Rees, H., Kozma-Bognar, L., Hall, A.J., and Locke, J.C. (2018). Coordination of robust single cell rhythms in the Arabidopsis circadian clock via spatial waves of gene expression. *Elife* *7*, e31700. <https://doi.org/10.7554/eLife.31700>.

Greenwood, M., Domijan, M., Gould, P.D., Hall, A.J.W., and Locke, J.C.W. (2019). Coordinated circadian timing through the integration of local inputs in Arabidopsis thaliana. *PLOS Biol.* *17*, e3000407. <https://doi.org/10.1371/journal.pbio.3000407>.

Hazen, S.P., Schultz, T.F., Pruneda-Paz, J.L., Borevitz, J.O., Ecker, J.R., and Kay, S.A. (2005). LUX ARRHYTHMO encodes a Myb domain protein essential for circadian rhythms. *Proc. Natl. Acad. Sci. USA* *102*, 10387–10392. <https://doi.org/10.1073/pnas.0503029102>.

Herrero, E., Kolmos, E., Bujdoso, N., Yuan, Y., Wang, M., Berns, M.C., Uhlworm, H., Coupland, G., Saini, R., Jaskolski, M., et al. (2012). *EARLY FLOWERING4* recruitment of *EARLY FLOWERING3* in the nucleus sustains the Arabidopsis circadian clock. *Plant Cell* 24, 428–443. <https://doi.org/10.1105/tpc.111.093807>.

Hicks, K.A., Millar, A.J., Carré, I.A., Somers, D.E., Straume, M.D., Meeks-Wagner, R., and Kay, S.A. (1996). Conditional circadian dysfunction of the Arabidopsis early-flowering 3 mutant. *Science* 274, 790–792. <https://doi.org/10.1126/science.274.5288.790>.

Hsu, P.Y., Devisetty, U.K., and Harmer, S.L. (2013). Accurate timekeeping is controlled by a cycling activator in Arabidopsis. *Elife* 2, e00473. <https://doi.org/10.7554/eLife.00473>.

Huang, H., Alvarez, S., Bindbeutel, R., Shen, Z., Naldrett, M.J., Evans, B.S., Briggs, S.P., Hicks, L.M., Kay, S.A., and Nusinow, D.A. (2016). Identification of Evening Complex associated proteins in Arabidopsis by affinity purification and mass spectrometry. *M. Cell. Proteomics* 15, 201–217. <https://doi.org/10.1074/mcp.M115.054064>.

Huang, W., Pérez-García, P., Pokhilko, A., Millar, A.J., Antoshechkin, I., Riechmann, J.L., and Mas, P. (2012). Mapping the core of the Arabidopsis circadian clock defines the network structure of the oscillator. *Science* 336, 75–79. <https://doi.org/10.1126/science.1219075>.

Hughes, M.E., Hogenesch, J.B., and Kornacker, K. (2010). JTK_CYCLE: An Efficient Nonparametric Algorithm for Detecting Rhythmic Components in Genome-Scale Data Sets. *J. Biol. Rhythms* 25, 372–380. <https://doi.org/10.1177/0748730410379711>.

James, A.B., Monreal, J.A., Nimmo, G.A., Kelly, C.L., Herzyk, P., Jenkins, G.I., and Nimmo, H.G. (2008). The circadian clock in Arabidopsis roots is a simplified slave version of the clock in shoots. *Science* 322, 1832–1835. <https://doi.org/10.1126/science.1161403>.

Katari, M.S., Nowicki, S.D., Aceituno, F.F., Nero, D., Kelfer, J., Thompson, L.P., Cabello, J.M., Davidson, R.S., Goldberg, A.P., Shasha, D.E., et al. (2010). VirtualPlant: A software platform to support systems biology research. *Plant Physiol.* 152, 500–515. <https://doi.org/10.1104/pp.109.147025>.

Kennaway, D., Boden, M., and Varcoe, T. (2012). Circadian rhythms and fertility. *Mol. Cell. Endocrinol.* 349, 56–61. <https://doi.org/10.1016/J.MCE.2011.08.013>.

Kim, D., Paggi, J.M., Park, C., Bennett, C., and Salzberg, S.L. (2019). Graph-based genome alignment and genotyping with HISAT2 and HISAT-genotype. *Nat. Biotechnol.* 37, 907–915. <https://doi.org/10.1038/s41587-019-0201-4>.

Kinmonth-Schultz, H.A., Golembeski, G.S., and Imaizumi, T. (2013). Circadian clock-regulated physiological outputs: Dynamic responses in nature. *Semin. Cell Dev. Biol.* 24, 407–413. <https://doi.org/10.1016/j.semcdb.2013.02.006>.

- Klepikova, A. V., Kasianov, A.S., Gerasimov, E.S., Logacheva, M.D., and Penin, A.A. (2016). A high resolution map of the *Arabidopsis thaliana* developmental transcriptome based on RNA-seq profiling. *Plant J.* 88, 1058–1070. <https://doi.org/10.1111/TPJ.13312>.
- Ma, Y., Gil, S., Grasser, K.D., and Mas, P. (2018). Targeted recruitment of the basal transcriptional machinery by LNK clock components controls the circadian rhythms of nascent RNAs in *Arabidopsis*. *Plant Cell* 30, 907–924. <https://doi.org/10.1105/tpc.18.00052>.
- Martínez-Fernández, I., Sanchís, S., Marini, N., Balanzá, V., Ballester, P., Navarrete-Gómez, M., Oliveira, A.C., Colombo, L., and Ferrándiz, C. (2014). The effect of NGATHA altered activity on auxin signaling pathways within the *Arabidopsis* gynoecium. *Front. Plant Sci.* 5, 210. <https://doi.org/10.3389/FPLS.2014.00210>.
- Más, P., Alabadi, D., Yanovsky, M.J., Oyama, T., and Kay, S.A.. (2003a). Dual role of TOC1 in the control of circadian and photomorphogenic responses in *Arabidopsis*. *Plant Cell* 15, 223–236. <https://doi.org/10.1105/tpc.006734>.
- Más, P., Kim, W.Y., Somers, D.E., and Kay, S.A. (2003b). Targeted degradation of TOC1 by ZTL modulates circadian function in *Arabidopsis thaliana*. *Nature* 426, 567–570. <https://doi.org/10.1038/nature02163>.
- McClung, C.R. (2019). The plant circadian oscillator. *Biology* 8, 14. <https://doi.org/10.3390/biology8010014>.
- Michael, T.P., Mockler, T.C., Breton, G., McEntee, C., Byer, A., Trout, J.D., Hazen, S.P., Shen, R., Priest, H.D., Sullivan, C.M., et al. (2008). Network discovery pipeline elucidates conserved time-of-day-specific cis-regulatory modules. *PLoS Genet.* 4, e14. <https://doi.org/10.1371/journal.pgen.0040014>.
- Millar, A.J., Carre, I.A., Strayer, C.A., Chua, N.H., and Kay, S.A. (1995). Circadian clock mutants in *Arabidopsis* identified by luciferase imaging. *Science* 267, 1161–1163. <https://doi.org/10.1126/science.7855595>.
- Mockler, T.C., Michael, T.P., Priest, H.D., Shen, R., Sullivan, C.M., Givan, S.A., McEntee, C., Kay, S.A., and Chory, J. (2007). The DIURNAL project: DIURNAL and circadian expression profiling, model-based pattern matching, and promoter analysis. *Cold Spring Harb. Symp. Quant. Biol.* 72, 353–363. <https://doi.org/10.1101/sqb.2007.72.006>.
- Mong, J., Baker, F., Mahoney, M., Paul, K., Schwartz, M., Semba, K., and Silver, R. (2011). Sleep, rhythms, and the endocrine brain: influence of sex and gonadal hormones. *J. Neurosci.* 31, 16107–16116. <https://doi.org/10.1523/JNEUROSCI.4175-11.2011>.
- Müller, A. (1961). Zur Charakterisierung der Blüten und Infloreszenzen von *Arabidopsis thaliana* (L.) Heynh. *Kulturpflanze* 9, 364–393. <https://doi.org/10.1007/BF02095757>.

Muroya, M., Oshima, H., Kobayashi, S., Miura, A., Miyamura, Y., Shiota, H., Onai, K., Ishiura, M., Manabe, K., and Kutsuna, S. (2021). Circadian Clock in *Arabidopsis thaliana* Determines Flower Opening Time Early in the Morning and Dominantly Closes Early in the Afternoon. *Plant Cell Physiol.* 62, 883-893. <https://doi.org/10.1093/pcp/pcab048>.

Nagel, D.H., and Kay, S.A. (2012). Complexity in the wiring and regulation of plant circadian networks. *Curr. Biol.* 22, R648–R657. <https://doi.org/10.1016/j.cub.2012.07.025>.

Nakamichi, N. (2020). The transcriptional network in the arabidopsis circadian clock system. *Genes* 11, 1284. <https://doi.org/10.3390/genes11111284>.

Nakamichi, N., Kita, M., Ito, S., Yamashino, T., and Mizuno, T. (2005). PSEUDO-RESPONSE REGULATORS, PRR9, PRR7 and PRR5, together play essential roles close to the circadian clock of *Arabidopsis thaliana*. *Plant Cell Physiol.* 46, 686–698. <https://doi.org/10.1093/pcp/pci086>.

Okada, M., and Mas, P. (2022). In Vivo Bioluminescence Analyses of Circadian Rhythms in *Arabidopsis thaliana* Using a Microplate Luminometer. *Methods Mol. Biol.* 2482, 395–406. https://doi.org/10.1007/978-1-0716-2249-0_27.

Perales, M., and Más, P. (2007). A functional link between rhythmic changes in chromatin structure and the *Arabidopsis* biological clock. *Plant Cell* 19, 2111–2123. <https://doi.org/10.1105/tpc.107.050807>.

Raven, J.A., and Griffiths, H. (2015). Photosynthesis in reproductive structures: costs and benefits. *J. Exp. Bot.* 66, 1699–1705. <https://doi.org/10.1093/JXB/ERV009>.

Rawat, R., Takahashi, N., Hsu, P.Y., Jones, M.A., Schwartz, J., Salemi, M.R., Phinney, B.S., and Harmer, S.L. (2011). REVEILLE8 and PSEUDO-RESPONSE REGULATOR5 form a negative feedback loop within the arabidopsis circadian clock. *PLoS Genet.* 7, e1001350. <https://doi.org/10.1371/journal.pgen.1001350>.

Robinson, J.T., Thorvaldsdottir, H., Winckler, W., Guttman, M., Lander, E.S., Getz, G., and Mesirov, J.P. (2011). Integrative genomics viewer. *Nat. Biotech.* 29, 24–26. <https://doi.org/10.1038/nbt.1754>.

Rugnone, M.L., Sovarna, A.F., Sanchez, S.E., Schlaen, R.G., Hernando, C.E., Seymour, D.K., Mancini, E., Chernomoretz, A., Weigel, D., Mas, P., et al. (2013). LNK genes integrate light and clock signaling networks at the core of the *Arabidopsis* oscillator. *Proc. Natl. Acad. Sci. U. S. A.* 110, 12120-12125. <https://doi.org/10.1073/pnas.1302170110>.

Sablowski, R. (2015). Control of patterning, growth, and differentiation by floral organ identity genes. *J. Exp. Bot.* 66, 1065–1073. <https://doi.org/10.1093/jxb/eru514>.

Salomé, P.A., and McClung, C.R. (2005). PSEUDO-RESPONSE REGULATOR 7 and 9 are partially redundant genes essential for the temperature responsiveness of the *Arabidopsis* circadian clock. *Plant Cell* 17, 791–803. <https://doi.org/10.1105/tpc.104.029504>.

Sanchez-Villarreal, A., Shin, J., Bujdoso, N., Obata, T., Neumann, U., Du, S.-X., Ding, Z., Davis, A.M., Shindo, T., Schmelzer, E., et al. (2013). TIME FOR COFFEE is an essential component in the maintenance of metabolic homeostasis in *Arabidopsis thaliana*. *Plant J.* 76, 188–200. <https://doi.org/10.1111/tpj.12292>.

Sanchez, S.E., and Kay, S.A. (2016). The Plant Circadian Clock: From a Simple Timekeeper to a Complex Developmental Manager. *Cold Spring Harb. Perspect. Biol.* 8, a027728. <https://doi.org/10.1101/cshperspect.a027748>.

Seo, P.J., and Mas, P. (2014). Multiple layers of posttranslational regulation refine circadian clock activity in *Arabidopsis*. *Plant Cell* 26, 79–87. <https://doi.org/10.1105/tpc.113.119842>.

Shalit-Kaneh, A., Kumimoto, R.W., Filkov, V., and Harmer, S.L. (2018). Multiple feedback loops of the *Arabidopsis* circadian clock provide rhythmic robustness across environmental conditions. *Proc. Natl. Acad. Sci.* 115, 7147–7152. <https://doi.org/10.1073/pnas.1805524115>.

Shim, J.S., Kubota, A., and Imaizumi, T. (2017). Circadian clock and photoperiodic flowering in *Arabidopsis*: CONSTANS is a Hub for Signal integration. *Plant Physiol.* 173, 5–15. <https://doi.org/10.1104/pp.16.01327>.

Simonini, S., and Østergaard, L. (2019). Female reproductive organ formation: A multitasking endeavor. *Curr. Top. Dev. Biol.* 131, 337–371. <https://doi.org/10.1016/bs.ctdb.2018.10.004>.

Smyth, D.R., Bowman, J.L., and Meyerowitz, E.M. (1990). Early flower development in *Arabidopsis*. *Plant Cell* 2, 755–767. <https://doi.org/10.2307/3869174>.

Sorkin, M.L., and Nusinow, D.A. (2021). Time Will Tell: Intercellular Communication in the Plant Clock. *Trends Plant Sci.* 26, 706–719. <https://doi.org/10.1016/j.tplants.2020.12.009>.

Takahashi, J.S. (2017). Transcriptional architecture of the mammalian circadian clock. *Nat. Rev. Genet.* 18, 164–179. <https://doi.org/10.1038/nrg.2016.150>.

Takahashi, N., Hirata, Y., Aihara, K., and Mas, P. (2015). A Hierarchical Multi-oscillator Network Orchestrates the *Arabidopsis* Circadian System. *Cell* 163, 148–159. <https://doi.org/10.1016/j.cell.2015.08.062>.

Thain, S.C., Hall, A., and Millar, A.J. (2000). Functional independence of circadian clocks that regulate plant gene expression. *Curr. Biol.* 10, 951–956. [https://doi.org/10.1016/S0960-9822\(00\)00630-8](https://doi.org/10.1016/S0960-9822(00)00630-8).

Thain, S.C., Murtas, G., Lynn, J.R., McGrath, R.B., and Millar, A.J. (2002). The circadian clock that controls gene expression in *Arabidopsis* is tissue specific. *Plant Physiol.* 130, 102–110. <https://doi.org/10.1104/pp.005405>.

Thorvaldsdóttir, H., Robinson, J.T., and Mesirov, J.P. (2013). Integrative Genomics Viewer (IGV): high-performance genomics data visualization and exploration. *Brief. Bioinform.* 14, 178–192.

<https://doi.org/10.1093/bib/bbs017>.

Wang, Z.Y., and Tobin, E.M. (1998). Constitutive expression of the CIRCADIAN CLOCK ASSOCIATED 1 (CCA1) gene disrupts circadian rhythms and suppresses its own expression. *Cell* 93, 1207–1217. [https://doi.org/10.1016/S0092-8674\(00\)81464-6](https://doi.org/10.1016/S0092-8674(00)81464-6).

Wang, Y., Wu, J.-F.F., Nakamichi, N., Sakakibara, H., Nam, H.-G.G., and Wu, S.-H.H. (2011). LIGHT-REGULATED WD1 and PSEUDO-RESPONSE REGULATOR9 form a positive feedback regulatory loop in the Arabidopsis circadian clock. *Plant Cell* 23, 486–498. <https://doi.org/10.1105/tpc.110.081661>.

Weigel, D. (1995). The genetics of flower development: From floral induction to ovule morphogenesis. *Annu. Rev. Genet.* 29, 19–39. <https://doi.org/10.1146/annurev.ge.29.120195.000315>.

Wellmer, F., Bowman, J.L., Davies, B., Ferrándiz, C., Fletcher, J.C., Franks, R.G., Graciet, E., Gregis, V., Ito, T., Jack, T.P., et al. (2014). Flower development: Open questions and future directions. *Methods Mol. Biol.* 1110, 103–124. https://doi.org/10.1007/978-1-4614-9408-9_5.

Wenden, B., Toner, D.L.K., Hodge, S.K., Grima, R., and Millar, A.J. (2012). Spontaneous spatiotemporal waves of gene expression from biological clocks in the leaf. *Proc. Natl. Acad. Sci.* 109, 6757–6762. <https://doi.org/10.1073/pnas.1118814109>.

Wu, J.F., Wang, Y., and Wu, S.H. (2008). Two new clock proteins, LWD1 and LWD2, regulate arabidopsis photoperiodic flowering. *Plant Physiol.* 148, 948–959. <https://doi.org/10.1104/pp.108.124917>.

Wu, J.F., Tsai, H.L., Joanito, I., Wu, Y.C., Chang, C.W., Li, Y.H., Wang, Y., Hong, J.C., Chu, J.W., Hsu, C.P., et al. (2016). LWD-TCP complex activates the morning gene CCA1 in Arabidopsis. *Nat. Commun.* 7, 13181. <https://doi.org/10.1038/ncomms13181>.

Xie, Q., Wang, P., Liu, X., Yuan, L., Wang, L., Zhang, C., Li, Y., Xing, H., Zhi, L., Yue, Z., et al. (2014). LNK1 and LNK2 Are Transcriptional Coactivators in the Arabidopsis Circadian Oscillator. *Plant Cell Online* 26, 2843–2857. <https://doi.org/10.1105/tpc.114.126573>.

Yakir, E., Hilman, D., Kron, I., Hassidim, M., Melamed-Book, N., and Green, R.M. (2009). Posttranslational Regulation of CIRCADIAN CLOCK ASSOCIATED1 in the Circadian Oscillator of Arabidopsis. *Plant Physiol.* 150, 844–857. <https://doi.org/10.1104/pp.109.137414>.

Yakir, E., Hassidim, M., Melamed-Book, N., Hilman, D., Kron, I., and Green, R.M. (2011). Cell autonomous and cell-type specific circadian rhythms in Arabidopsis. *Plant J.* 68, 520–531. <https://doi.org/10.1111/j.1365-313X.2011.04707.x>.

Yamaguchi, N., Winter, C.M., Wu, M.-F., Kwon, C.S., William, D.A., and Wagner, D. (2014). PROTOCOLS: Chromatin Immunoprecipitation from Arabidopsis Tissues. *Arabidopsis Book* 12,

e0170. <https://doi.org/10.1199/tab.0170>.

Young, M.W., and Kay, S.A. (2001). Time zones: a comparative genetics of circadian clocks. *Nat. Rev. Gen.* 2, 702–715. <https://doi.org/10.1038/35088576>.

Zielinski, T., Moore, A.M., Troup, E., Halliday, K.J., and Millar, A.J. (2014). Strengths and Limitations of Period Estimation Methods for Circadian Data. *PLoS One* 9, e96462. <https://doi.org/10.1371/journal.pone.0096462>.

Zúñiga-Mayo, V.M., Gómez-Felipe, A., Herrera-Ubaldo, H., and De Folter, S. (2019). Gynoecium development: Networks in Arabidopsis and beyond. *J. Exp. Bot.* 70, 1447–1460. <https://doi.org/10.1093/jxb/erz026>.